Research Paper

Apelin protects against ischemia-reperfusion injury in diabetic myocardium via inhibiting apoptosis and oxidative stress through PI3K and p38-MAPK signaling pathways

Songtao An[1], Xi Wang[1], Huairui, Shi[2], Xueqiang Zhang[3], Hua Meng[1], Wenbo Li[1], Dongchang Chen[1], Junbo Ge[2]

[1]Department of Cardiology, Henan Province People's Hospital, People's Hospital of Zhengzhou University, Zhengzhou 450003, Henan, China
[2]Department of Cardiology, Zhongshan Hospital, Fudan University, Shanghai 200032, China
[3]Department of Cardiology, Hongxing Hospital, Hami 839000, Xinjiang, China

Correspondence to: Junbo Ge; **email:** ge.junbo@zs-hospital.sh.cn

ABSTRACT

Among all diabetes mellitus-associated cardiovascular diseases, morbidity of diabetic myocardium with ischemia reperfusion injury (D-IRI) is increasing year by year. We aimed to discover a therapeutic biomarker and investigate its mechanism in D-IRI. High-fat diet and streptozotocin-induced diabetes rats were operated with IRI or sham. Recombined lentiviral vector encoding Apelin was injected into D-IRI rat via tail vein. Cardiac function, infarct size, cellular death and oxidative stress were major outcome measures. Cardiomyocyte ischemia reperfusion injury was more serious in D-IRI rats than in non-diabetes ischemia reperfusion injury (ND-IRI) rats. The secretion of NTproBNP was increased in D-IRI compared with ND-IRI. Bcl-2 expression was decreased, and Bax and cleaved caspase-3 expression was increased in D-IRI rats compared with ND-IRI rats, which were reversed after treatment with Apelin. Apelin-upregulation improved cardiomyocyte ischemia reperfusion injury and decreased NT-proBNP levels in D-IRI rats. Apelin overexpression enhanced PI3K and eNOS levels while reduced those of p38-MAPK and iNOS in D-IRI rats. Apelin overexpression protected against D-IRI through inhibiting apoptosis and oxidative stress via PI3K and p38MAPK signaling pathways in D-IRI rats. These findings provide critical new insight into understanding of Apelin's cardio-protective effects, which may become a novel therapeutic target for the diabetic IRI patients.

INTRODUCTION

Diabetes mellitus (DM) is a metabolic syndrome. Epidemiological discoveries show that the DM is the most vital risk factor for the myocardial, the cardiovascular disorders, and the ischemia reperfusion injury (IRI), and the mortality in these diseases is 2 to 6 times higher in the DM patients compared to the non-DM patients [1]. Yin, et al. found that the poor prognosis of DM is at least partly correlated with the endogenous cardio-protective strategies in DM, for example, the ischemia reperfusion injuries (IRI) [2]. IRI mainly occurs an acute ST-segment elevation myocardial infarction in patients who have experienced either thrombolytic therapy or primary percutaneous coronary intervention (PPCI) for reducing acute myocardial ischemic injury and limiting the size of myocardial infarction. However, the myocardial reperfusion always evokes myocardial reperfusion injury [3, 4]. Therefore, we believed that establishment of an effective strategy decreasing the degree of infarction in the process of IRI is pretty significant in clinical cases.

The chaos of renal-angiotensin system (RAS) is associated with initiation of cardiovascular disorder [5]. Angiotensin II (Ang II), the main regulator of RAS, regulates and activates Angiotensin II type 1 (AT1) and the reduced form of NADPH oxidase to trigger superoxide anion. Additionally, NO and oxidize tetrahydrobiopterin (BH_4) can interact with superoxide anion and peroxynitrite. The endothelial nitric oxide synthase (eNOS) leads to uncoupling and then endothelial dysfunction-associated oxidative stress is emerged [6–8]. Apelin was firstly discovered from bovine stomach extracts in 1998, which is a novel adipocytokine secreted by the white adipose tissues and could bind to the Apelin receptor (APJ, orphan G protein-coupled receptor) with high affinity [9]. Apelin, activated under cardiovascular injury or disorder, is a homologous molecule of Ang II and belongs to the RAS [10, 11]. Gurzu et al. reported that the Apelin restrains the Ang II-mediated vasoconstriction via binding to the Apelin receptor (APJ) [12]. The RAS regulates the cardiovascular system, kidney system, and blood pressure [13]. Apelin is distributed in several tissues and plays multiple bioactivities via combination with APJ through autocrine, paracrine and endocrine pathways [14–16]. The decrease of arterial pressure induced by Apelin is largely attributed to the activation of eNOS [17]. The angiotensin converting enzyme 2 (ACE2) is a negative modulator of the RAS, and Apelin knock-down could suppress the expression of ACE2 [18, 19]. The Apelin signaling system is implicated in various physiological effects and participates in multiple pathological processes, especially in the cardiovascular disorders (such as heart failure, hypertension, myocardial injury, atherosclerosis), diabetes complicated with microvascular diseases, tumors, ischemia reperfusion injuries, as well as the pre-eclampsia [20]. Large number of studies indicated that increased angiogenesis offers oxygen and nutrients to ischemia area of myocardium. W. Wang, et al. and S. Kumagai, et al. published that Apelin promotes angiogenesis in myocardial infarction (MI) [21, 22]. Furthermore, Apelin-13 enhances the expression of vascular endothelial growth factor (VEGF), VEGF receptor-2 (VEGFR-2) and eNOS, enhancing the capillary density in the heart of MI rat [23].

However, there are also some un-resolved problems in the diabetic myocardium with ischemia reperfusion injury (D-IRI) injury. Firstly, specific mechanism of the D-IRI has not been fully clarified. Secondly, effectively therapeutic strategies for D-IRI still need better investigation. Therefore, the present study utilized D-IRI rat model to explore potential therapeutic strategy and related mechanisms of Apelin in D-IRI injury.

RESULTS

Establishment of animal models

In T2DM rat model, rats were successfully established as DM. Twenty-four of thirty-seven rats were established as DM complicated with IRI (D-IRI), and six of eight rats were established as diabetic control (D-sham). Twenty-four of thirty rats were established as IRI (ND-IRI), and seven of eight rats were established as control (ND-sham).

Cardiac function was significantly injured in D-IRI rats

The cardiac function of rats in different groups was evaluated by ultrasonic inspection the 6th week after IRI surgery. The results indicated that the LVIDd, LVIDs and the LVPWs were increased significantly, while the EF and FS were decreased significantly in the ND-IRI and D-IRI groups compared to ND-Sham and D-Sham groups, respectively (Table 1). Besides, LVIDd, LVIDs, LVPWs were increased markedly and the EF and FS were decreased markedly in D-IRI group compared to ND-IRI group (Table 1, P<0.01). Eight weeks after surgery, the hemodynamic parameters were evaluated (Table 2). The results displayed that the LVEDP was increased distinctly while LVSP and LVDP/dtmax were decreased distinctly in the ND-IRI and D-IRI groups compared to ND-Sham and D-Sham groups, respectively. Besides, the LVEDP was increased but LVSP and LVDP/dtmax were decreased significantly in D-IRI group compared to ND-IRI group. Furthermore, significantly increased LVEDP as well as decreased LVSP and LVDP/dtmax were observed in D-Sham group compared to ND-Sham group. NT-proBNP is a marker of myocardial ischemia. The concentration of NT-proBNP in D-IRI and ND-IRI group was obviously promoted compared to D-Sham and ND-Sham groups, respectively. The concentration of NT-proBNP in D-IRI group was also promoted significantly relative to ND-IRI group. Moreover, the NT-proBNP was obviously enhanced in D-Sham group compared to ND-Sham group. In conclusion, rats with diabetes had bad cardiac function and myocardial ischemia/reperfusion aggravated these dysfunctions.

As shown in Figure 1A, 1B, TTC staining showed that the infarct size in D-IRI group was significantly increased compared to the ND-IRI group. Moreover, there was no obvious infarct field in ND-Sham and D-Sham groups. In the IR group, loss of myofibril, cardiomyocytes necrosis and abnormal structure emerged (Figure 1C). These results indicated that the cardiac function dramatically descended and the model was established successfully.

Table 1. Ultrasonic inspection results for rats.

Groups	ND-Sham (n=8)	ND-IRI (n=13)	D-IRI (n=14)	D-Sham (n=7)
LVIDd (mm)	6.45±0.38	10.21±0.67[*]	15.32±0.82[*$]	9.35±0.53[#]
LVIDs (mm)	2.98±0.57	6.16±0.38[*]	8.89±0.98[*$]	4.02±0.68[#]
EF (%)	67.58±4.69	50.73±5.36[*]	35.73±2.88[*$]	56.58±3.22[#]
FS (%)	50.13±6.31	29.82±6.21[*]	26.82±4.39[*]	40.13±4.35[#]
IVSd (mm)	1.04±0.25	1.33±0.59[*]	1.83±0.59[*$]	1.44±0.45[#]
IVSs (mm)	1.76±0.56	1.98±0.47	3.02±0.63	2.06±0.55[#]
LVPWd (mm)	1.73±0.26	1.99±0.17[*]	2.15±0.17	1.92±0.26[#]
LVPWs (mm)	1.58±0.25	2.28±0.10[*]	3.07±0.12[*]	2.47±0.35[#]

Data are presented as mean ± standard deviation. [*]P<0.05 represents the values compared to ND-Sham group. [#]P<0.05 represents the values compared to the ND-sham group. [$]P<0.05 represents the values compared to ND-IRI group. ND-Sham: Non-diabetes sham group; ND-IRI: Non-diabetes ischemia reperfusion injury; D-IRI: Diabetes ischemia reperfusion injury; D-Sham: Diabetes sham group.

Table 2. Cardiac hemodynamic in non-diabetic or diabetic rats with or without ischemia reperfusion.

Group	ND-Sham (n=8)	ND-IRI (n=13)	D-IRI (n=14)	D-Sham (n=7)
LVEDP (mmHg)[a]	3.76±0.42	10.24±0.78[*]	27.58±0.87[#]	6.22±0.32[*]
LVSP (mmHg)[a]	170.5±3.7	123.5±5.3[*]	98.8±3.1[#]	150.5±3.6[*]
LVdp/dtmax(mmHg/s)[a]	2959±69	2136±70[*]	1113±48[#]	1749±49[*]
NT-proBNP (pg/ml)[b]	50(21~289)	150(28~589)[*]	220(108~1589)[#]	450(128~2589)[*]

Data are presented as mean± standard deviation [a] and/or median (range)[b]. [*] P<0.05 versus ND-Sham, [#] P<0.05 versus D-Sham. ND-Sham: Non-diabetes sham group; ND-IRI: Non-diabetes ischemia reperfusion injury; D-IRI: Diabetes ischemia reperfusion injury; D-Sham: Diabetes sham group.
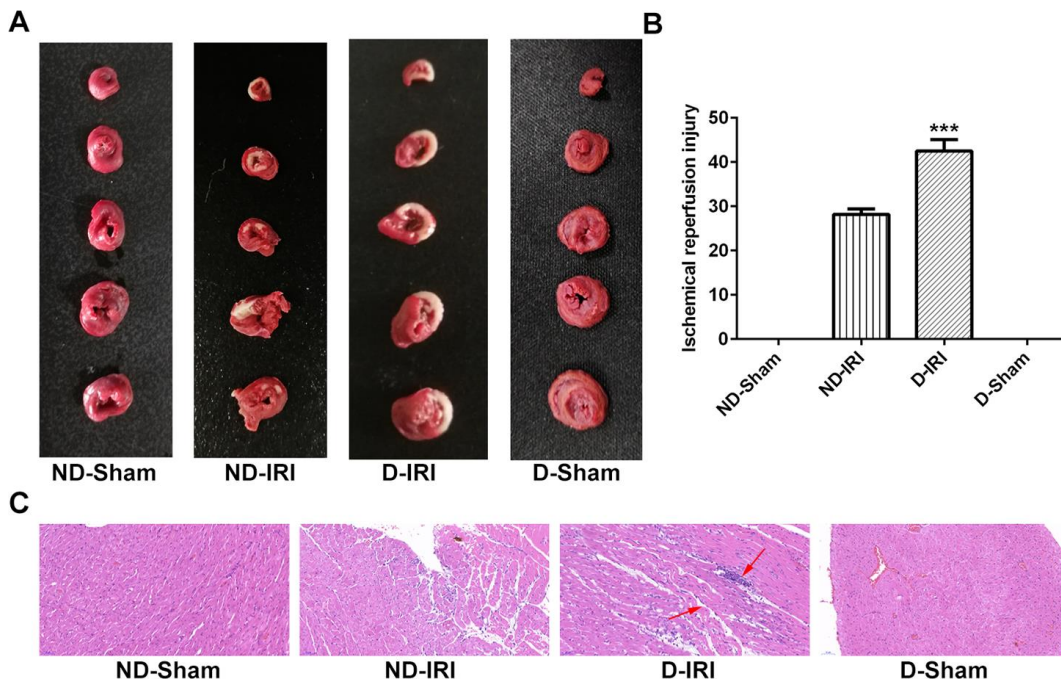

Figure 1. Examination for the cardiomyocyte's function in ischemia reperfusion (IR) injury. (**A**, **B**) The IR injury was detected by the TTC staining. P<0.001 compared to ND-IRI group. (**C**) The cardiac pathology was evaluated by HE staining. Magnification, ×200. TTC: triphenyltetrazoliu chloride; HE: Hematoxylin-eosin; ND-Sham: Non-diabetes sham group; ND-IRI: Non-diabetes ischemia reperfusion injury; D-IRI: Diabetes ischemia reperfusion injury; D-Sham: Diabetes sham group.

D-IRI injury associated with apoptosis

As shown in Figure 2A, apoptosis detected by TUNEL assay was observed in ND-IRI and D-IRI groups but not in ND-Sham and D-Sham groups, and D-IRI rats presented more significant increase of apoptosis level than ND-IRI rats. According to the above results, we speculated that the key biomarkers of apoptosis might participate in the pathological processes of D-IRI or ND-IRI. The expression of Bax, Bcl-2 and cleaved caspase-3 (activated form of caspase-3) was examined by RT-qPCR and western blot assays. The RT-qPCR results revealed that Bcl-2 was significantly reduced in ND-IRI and D-IRI groups compared to ND-Sham and D-Sham groups, respectively (Figure 2B). Meanwhile, the Bcl-2 expression in D-IRI group was remarkably decreased compared to ND-IRI group (Figure 2B, $P<0.001$). However, Bax and cleaved caspase-3 expression were remarkably increased in ND-IRI and D-IRI groups compared to ND-Sham and D-Sham groups, respectively. The expression changes in D-IRI group were more than those in ND-IRI group (Figure 2C). Moreover, the western blot assay also illustrated the same changes of Bcl-2, Bax and cleaved caspase-3 (Figure 2C). These results indicated that apoptosis might be involved in D-IRI.

Alteration of Apelin levels in myocardial tissues and serum in D-IRI and ND-IRI rats

In order to discover a biomarker that triggers the diabetic myocardial ischemia reperfusion injury, the cardiovascular disease-related protein, Apelin, was examined in both myocardial tissues and serum. In the former two weeks, the expression levels of Apelin in myocardium tissues were increased in ND-IRI and D-IRI groups compared with ND-Sham and D-Sham groups (Figure 3A). Also, the Apelin levels were expressed more in D-IRI group than in ND-IRI group (Figure 3A). However, the Apelin expression in ND-IRI, D-Sham and D-IRI was significantly lowered from the fourth week (Figure 3A). Meanwhile, the blood samples were used to detect expression level of Apelin in serum, which illustrated the similar changes to myocardial tissues. However, the decrease of Apelin in serum was delayed for two weeks compared to myocardial tissues (Figure 3B).

Apelin improved cardiac function for D-IRI rats

The ultrasonic inspection was performed 6 weeks after surgery. The results unveiled that the LVIDd, LVIDs and LVPWs were significantly higher, whereas the EF and FS were significantly lower in the D-IRI control group and Ad-GFP group compared to the D-Sham group (Table 3). Further, the LVIDd, LVIDs, and LVPWs were significantly lower, and the EF and FS were significantly higher in Ad-Apelin compared to Ad-GFP group (Table 3).

After the injection of the Ad-Apelin, the hemodynamic parameters, including LVEDP, LVSP and LVdp/dtmax, were assessed. IRI injury significantly increased the LVEDP and decreased LVSP and LVdp/dtmax levels in D-IRI and Ad-GFP groups compared to D-Sham group (Table 4). The results indicated that the LVEDP was decreased notably in Ad-Apelin group compared to Ad-GFP group (Table 4). Meanwhile, the LVSP and LVdp/dtmax were increased notably in Ad-Apelin group in comparison with the D-IRI control group and Ad-GFP group (Table 4). Test of NT-proBNP unmasked that the NT-proBNP levels were decreased markedly compared to D-IRI control group and Ad-GFP group (Table 4). Furthermore, the indexes for IRI, including IRI size and heart weight index, were also evaluated. The results discovered that the IRI size in myocardial tissues of Ad-Apelin group was significantly less than those of D-IRI control and Ad-GFP groups (Figure 4A, 4B). Meanwhile, the heart weight index was also decreased in Ad-Apelin group compared to Ad-GFP group (Table 4). In the IR group, Apelin administration reversed the D-IRI injury on the loss of myofibril, cardiomyocytes necrosis and abnormal structure (Figure 4C).

Apelin enhanced PPAR levels and decreased collagen volume fraction (CVF) value in myocardial tissues

To investigate the protective role of Apelin in cardiovascular diseases, the PPAR-alpha and CVF were examined in the myocardial tissues. The results exhibited that the PPAR-alpha expression was dramatically elevated in the Ad-Apelin group relative to the Ad-GFP group (Figure 5A). The Masson's stain evaluated the myocardial fibrosis level, and CVF value was significantly lessened in the Ad-Apelin group in contrast to Ad-GFP group (Figure 5B, 5C).

Apelin inhibited apoptosis in D-IRI injury

In order to investigate the mechanism of the protective function of Apelin on the myocardial tissues, the apoptosis level and apoptotic biomarkers, such as Bax, Bcl-2 and cleaved caspase-3, were examined by the TUNEL, RT-qPCR and western blot assays, respectively. The TUNEL staining results indicated the reduced apoptotic index in Ad-Apelin group compared to Ad-GFP group (Figure 6A, 6B). The western blot analysis results indicated that the levels of Bax and cleaved caspase-3 were significantly declined, and Bcl-2 levels were significantly elevated compared to the Ad-

GFP group (Figure 6C, 6D). Likewise, in RT-qPCR analysis, the decrease of Bcl-2 and increase of cleaved caspase-3 in D-IRI group and Ad-GFP group compared to D-Sham group were viewed, whereas the cleaved caspase-3 expression was inhibited after administration of Ad-Apelin (Figure 6E). Although the gene alteration of Bax and Bcl-2 was not significant in some groups, the increase or decrease trend was similar to protein changes.

Apelin played roles in a few signaling pathways

To clarify the specific pathway by which the Apelin protected against the IRI, the PI3K, p38MAPK, eNOS and iNOS expression levels were examined using the western blot assay (Figure 7). The PI3K levels were significantly enhanced in Apelin group compared to the GFP group. Furthermore, the p38MAPK and iNOS expression was repressed in Apelin group compared to GFP group.
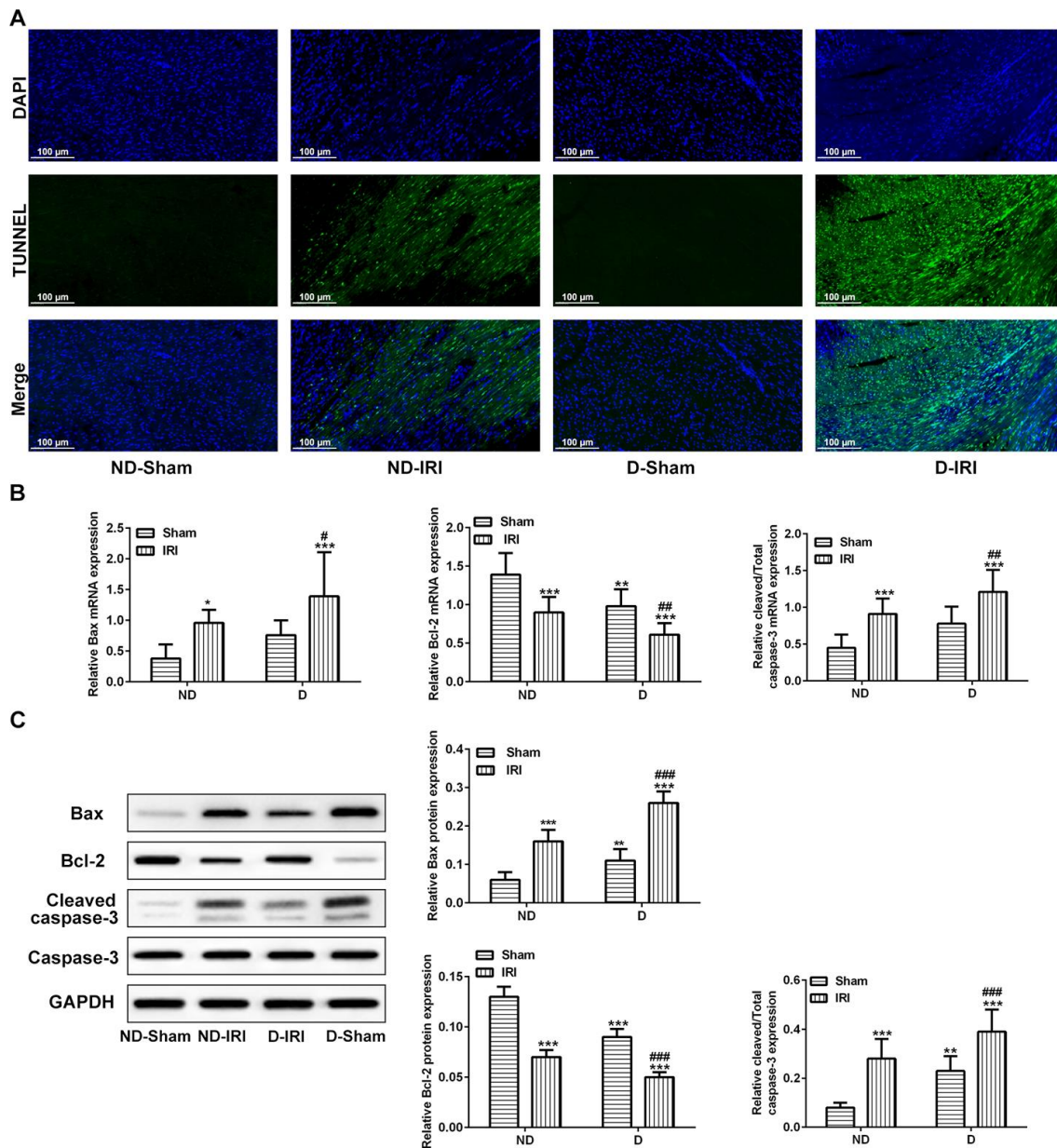

Figure 2. Observation for the apoptosis and associated biomarkers. (**A**) Apoptosis in myocardium was determined by TUNEL analysis. Scale bar=50 μm. (**B**) mRNA levels of Bcl-2, Bax, and cleaved caspase-3 detecting by RT-qPCR. *P<0.05, **P<0.01, ***P<0.001 represents the values compared to the ND-Sham group; $^{#}$P<0.05, $^{##}$P<0.01 represents the values compared to D-Sham. (**C**) Protein levels of Bcl-2, Bax, and cleaved caspase-3 detecting by western blot assay. **P<0.01, ***P<0.001 represents the values compared to the ND-Sham group; $^{###}$P<0.001 represents the values compared to D-Sham. ND-Sham: Non-diabetes sham group; ND-IRI: Non-diabetes ischemia reperfusion injury; D-IRI: Diabetes ischemia reperfusion injury; D-Sham: Diabetes sham group.

DISCUSSION

The diabetes mellitus-caused cardiovascular diseases are the most important reasons for the higher mortality of humans, especially the type 2 diabetes mellitus [24]. Among these diseases, the morbidity of D-IRI is increasing with each passing year [25, 26]. The previous study [27] indicated that the diabetes mellitus can cause many dysfunction, endothelial dysfunction, insulin resistance, abnormal metabolism of myocardium included. In the recent years, it has been reported that the initial processes for the diabetic myocardial remodeling and the myocardial diastolic dysfunction generate cardiac insufficiency. Schannwell et al. [28] performed a large epidemiological investigation and discovered that the morbidity and mortality of cardiovascular diseases in diabetes mellitus patients are significantly higher compared with non-diabetic patients. Therefore, we established the diabetes mellitus

model and/or IRI model to compare the alterations of cardiac functions and apoptotic characteristics.

The ultrasonic inspection results showed that the LVIDd, VLIDs, LVPWs and LVEDP were increased significantly, but LVSP and LVdp/dtmax were significantly decreased in ND-IRI (or D-IRI) group compared to ND-Sham (or D-Sham) group. The result hinted that the chamber of heart was significantly enlarged, and that left ventricular systolic thickness significantly decreased. Meanwhile, the EF and FS were reduced markedly and LVEDP was increased significantly in IRI rats, suggesting that heart function decreased significantly. Meanwhile, LVIDd, VLIDs, and LVPWs were augmented, whereas the EF and FS were lessened significantly in D-IRI group compared to ND-IRI group. These results suggested that the heart failure was aggravated in the D-IRI rats compared to ND-IRI rats. Therefore, we believed that the symptoms
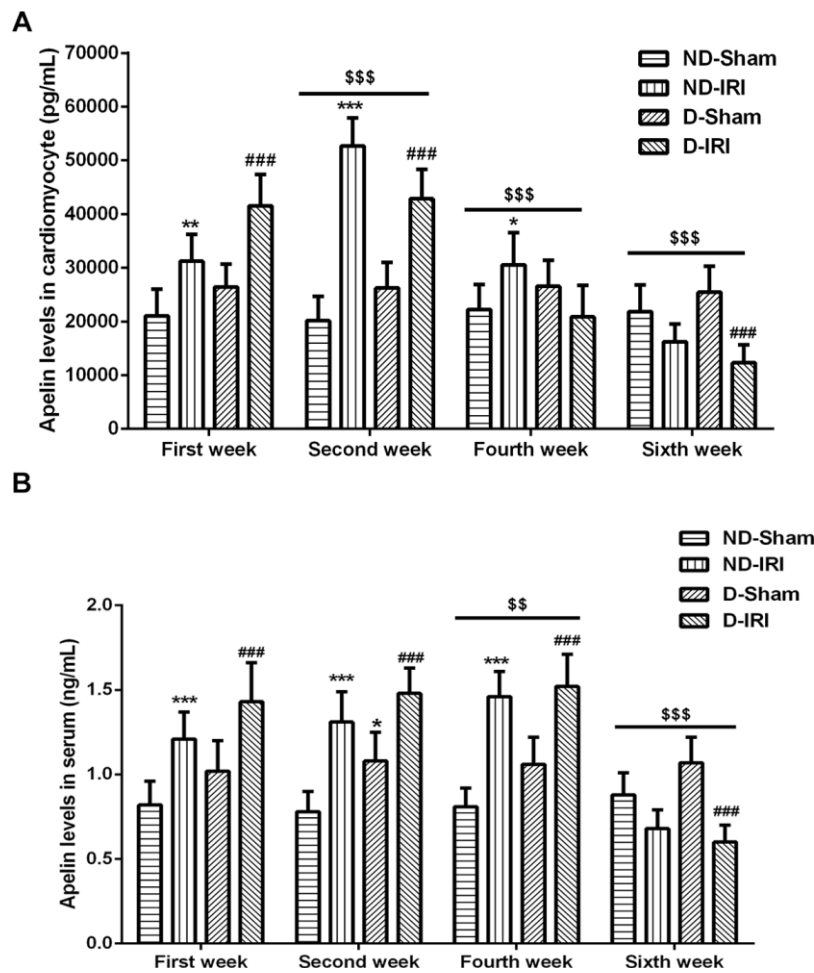

Figure 3. Evaluation for the levels of Apelin in diabetic- or no diabetic IRI rats. The levels of Apelin in both cardiomyocyte (**A**) and serum (**B**) were evaluated by ELISA kit. * P<0.05, ** P<0.01, *** P<0.001 represent the values compared to the ND-Sham group. ### P<0.001 represents the values compared to the D-Sham group. $$$ P<0.001 represents the values compared to the First week. ND-Sham: Non-diabetes sham group; ND-IRI: Non-diabetes ischemia reperfusion injury; D-IRI: Diabetes ischemia reperfusion injury; D-Sham: Diabetes sham group.

Table 3. Ultrasonic inspection results for the diabetes ischemia reperfusion injury rat models after Apelin therapy.

Group	D-Sham (n=7)	D-IRI (n=14)	Ad-GFP (n=6)	Ad-Apelin (n=6)
LVIDd (mm)	9.35±0.53	15.321±0.82[*]	14.88±0.86[*]	9.23±0.56[#]
LVIDs (mm)	4.02±0.68	8.89±0.98[*]	9.63±0.89[*]	4.22±0.68[#]
EF (%)	56.58±3.22	35.73±2.88[*]	35.43±3.96[*]	55.65±3.22[#]
FS (%)	40.13±4.35	26.82±4.39[*]	27.44±3.85[*]	39.31±3.87[#]
IVSd (mm)	1.44±0.45	1.83±0.59	1.98±0.55	1.49±0.48
IVSs (mm)	2.06±0.55	3.02±0.63	3.11.11±0.51	1.96±0.46
LVPWd (mm)	1.92±0.26	2.15±0.17	2.35±0.25	1.98±0.26
LVPWs (mm)	2.47±0.18	3.07±0.22[*]	3.01±0.20[*]	2.87±0.15[#]

[*] P<0.05 represents the values compared to the D-Sham group. [#] P<0.05 represents the values compared to Ad-GFP. D-Sham: Diabetes sham group. D-IRI: Diabetes ischemia reperfusion injury; Ad-GFP: D-IRI rats injecting Ad-recombined lentiviral vector expressing GFP. Ad-Apelin: D-IRI rats injecting Ad-recombined lentiviral rector expressing Apelin.

Table 4. Cardiac hemodynamic for the diabetes ischemia reperfusion injury rat models after Apelin therapy.

Group	D-Sham (n=7)	D-IRI (n=14)	Ad-GFP (n=6)	Ad-Apelin (n=6)
Body weight (g) [a]	248.1±4.1	255.1±3.8	250.2±3.8	255.6±3.9
Heart weight (g) [a]	1.041±0.049	1.682±0.051	1.692±0.041	1.208±0.045
HWI [a]	0.0041±0.0001	0.0066±0.0004[*]	0.0067±0.0004[*]	0.0047±0.0002[#]
LVEDP (mmHg)[a]	6.22±0.32	27.58±0.87[*]	28.44±0.98[*]	9.06±0.57[#]
LVSP (mmHg)[a]	150.5±3.6	98.8±3.1[*]	99.5±4.3[*]	146.7±4.66[#]
LVdp/dtmax(mmHg/s)[a]	1749±49	1113±48[*]	1256±40[*]	1819±64[#]
NT-proBNP[b]	450(128~2589)	220(108~1589)[*]	240(115~1789)[*]	450(128~2589)[#]

Data are presented as mean ± standard deviation [a] and/or median (range)[b]. [*] P<0.05 versus D-Sham, [#] P<0.05 versus Ad-GFP. HWI, heart weight index. D-Sham: Diabetes sham group. D-IRI: Diabetes ischemia reperfusion injury; Ad-GFP: D-IRI rats injecting Ad-recombined lentiviral vector expressing GFP. Ad-Apelin: D-IRI rats injecting Ad-recombined lentiviral rector expressing Apelin.
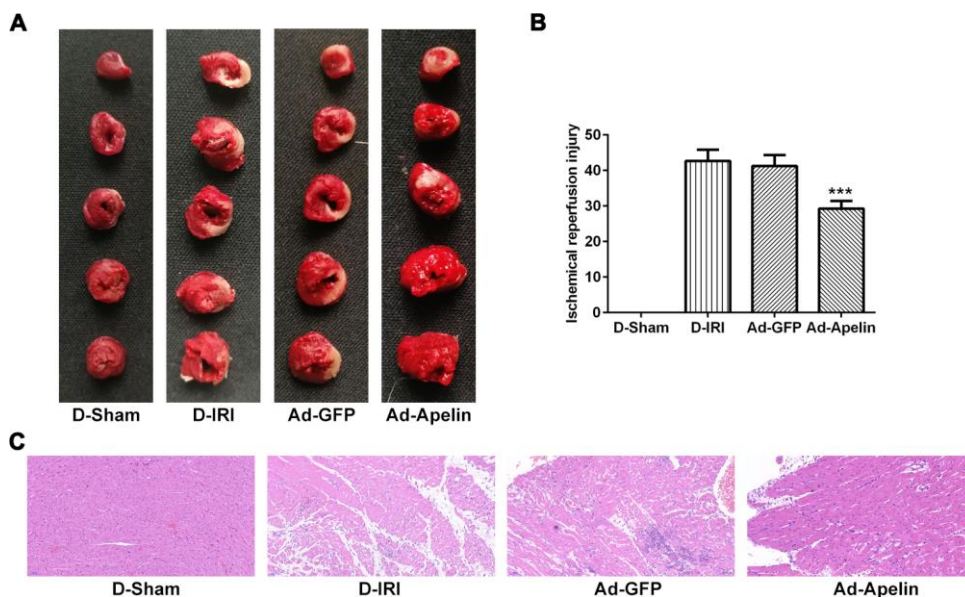

Figure 4. Role of Apelin on cardiac infarction and pathology in cardiac IRI rats. (**A**, **B**). The infarction of cardiac was evaluated by TTC staining. [***]P<0.001 versus D-IRI. (**C**) The pathology of myocardium was assessed by HE staining. Magnification, ×200. TTC: triphenyltetrazoliu chloride; HE: Hematoxylin-eosin; D-Sham: Diabetes sham group; D-IRI: Diabetes ischemia reperfusion injury; Ad-GFP: D-IRI rats injected with Ad-recombined lentiviral vector expressing GFP. Ad-Apelin: D-IRI rats injected with Ad-recombined lentiviral rector expressing Apelin.

of heart failure were more serious in D-IRI rats than ND-IRI rats.

Past studies [29, 30] have proved that the NT-proBNP is the optimized biomarker for the diagnosis of heart failure, and is the optimized biomarker for prognosis of cardiovascular diseases. The results indicated that NT-proBNP concentration in D-IRI group was markedly increased compared to D-Sham group but increased significantly compared to ND-IRI group. These findings hinted that the rats had developed the decreased cardiac functions before the formation of the cardiac infarcts in D-IRI rats. We speculated that the D-IRI caused high hypoxia, leading to the enlarged ventricle and increased secretion of NT-proBNP, consistent with the previous study [31].

Recently, researches [32, 33] have found that the apoptosis participates in processes of the physiological and pathological changes following with the development of study of cardiovascular diseases. Herein, we examined the key biomarkers [34], such

Bax, Bcl-2 and cleaved caspase-3 (activated form of caspase-3), by using RT-qPCR and western blot experiments. The changes of Bax and Bcl-2 illustrated that the hypoxia-ischemia induced in D-IRI rats and ND-IRI rats activated apoptosis. The mechanism of the apoptosis may be triggered by the oxidative stress and decreased mitochondrial potential, which sequentially induces the release of cytochrome C [35]. Subsequently, the cytochrome C provokes the cleavage of the caspase-3 to the activated form, cleaved caspase-3.

Apelin and its receptor, AJP, are extensively distributed in heart and the vascular tissues, both of which involve in various pathological processes, especially in the cardiovascular disorders, diabetes complicated with micro-vascular diseases and the ischemia reperfusion injuries [20]. Therefore, in this study, the levels of Apelin were raised significantly in the early stage of the IRI in both D-IRI rats and ND-IRI rats, but decreased in the medium stage. However, the Apelin levels increased to the peak values at one week post the operation. According to the above results, we speculated that the
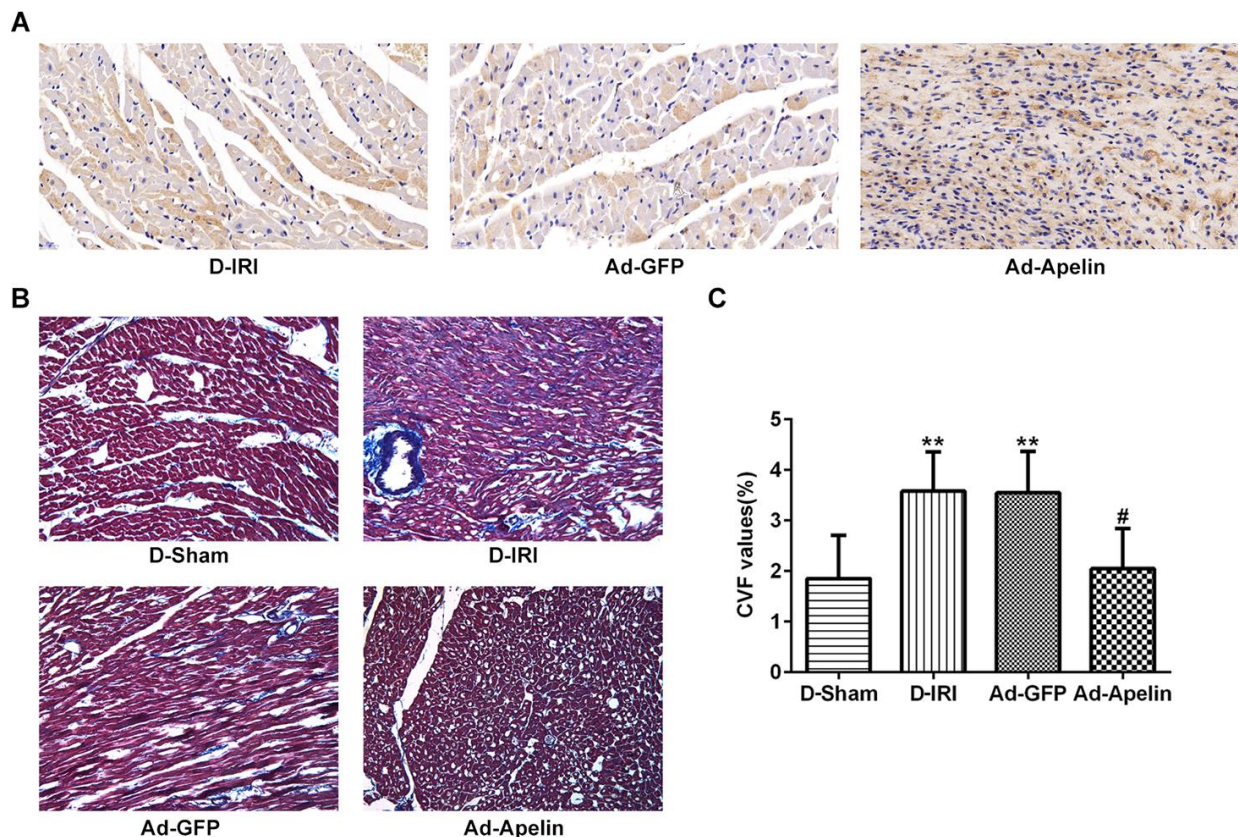

Figure 5. Impacts of Apelin on PPAR-alpha expression and CVF values in D-IRI rats. (**A**) Examination for PPAR-alpha expression by immunohistochemistry staining. Magnification, ×200. (**B**, **C**) CVF values in D-IRI rats was examined by Masson's staining. [**]P<0.01 represents the values compared to the D-Sham group. [#]P<0.05 represents the values compared to the Ad-GFP group. Magnification, ×200. CVF: collagen volume fraction; D-Sham: Diabetes sham group; D-IRI: Diabetes ischemia reperfusion injury; Ad-GFP: D-IRI rats injected with Ad-recombined lentiviral vector expressing GFP. Ad-Apelin: D-IRI rats injected with Ad-recombined lentiviral rector expressing Apelin.

diabetes and/or IRI-induced hypoxia-ischemia activated and the metabolic disturbance seriously upregulated the expression of the Apelin, and aggravated the cardiac function quickly. Our result was consistent with the previous study [36], showing that the Apelin played an important role in the early stage of heart failure. Thus, the expression of Apelin might be associated with the oxidative stress or apoptosis in the myocardial tissues. Considering all of the above results in both D-IRI and ND-IRI rats, including enlarged infarct size, enhanced

apoptosis, decreased Apelin levels in D-IRI rats compared to ND-IRI rats, we concluded that the cardiac function in D-IRI rats was more serious compared to the ND-IRI rats. Therefore, in the following study, we mainly investigated the effects of exogenously expressed Apelin on the cardiac function and the associated indexes.

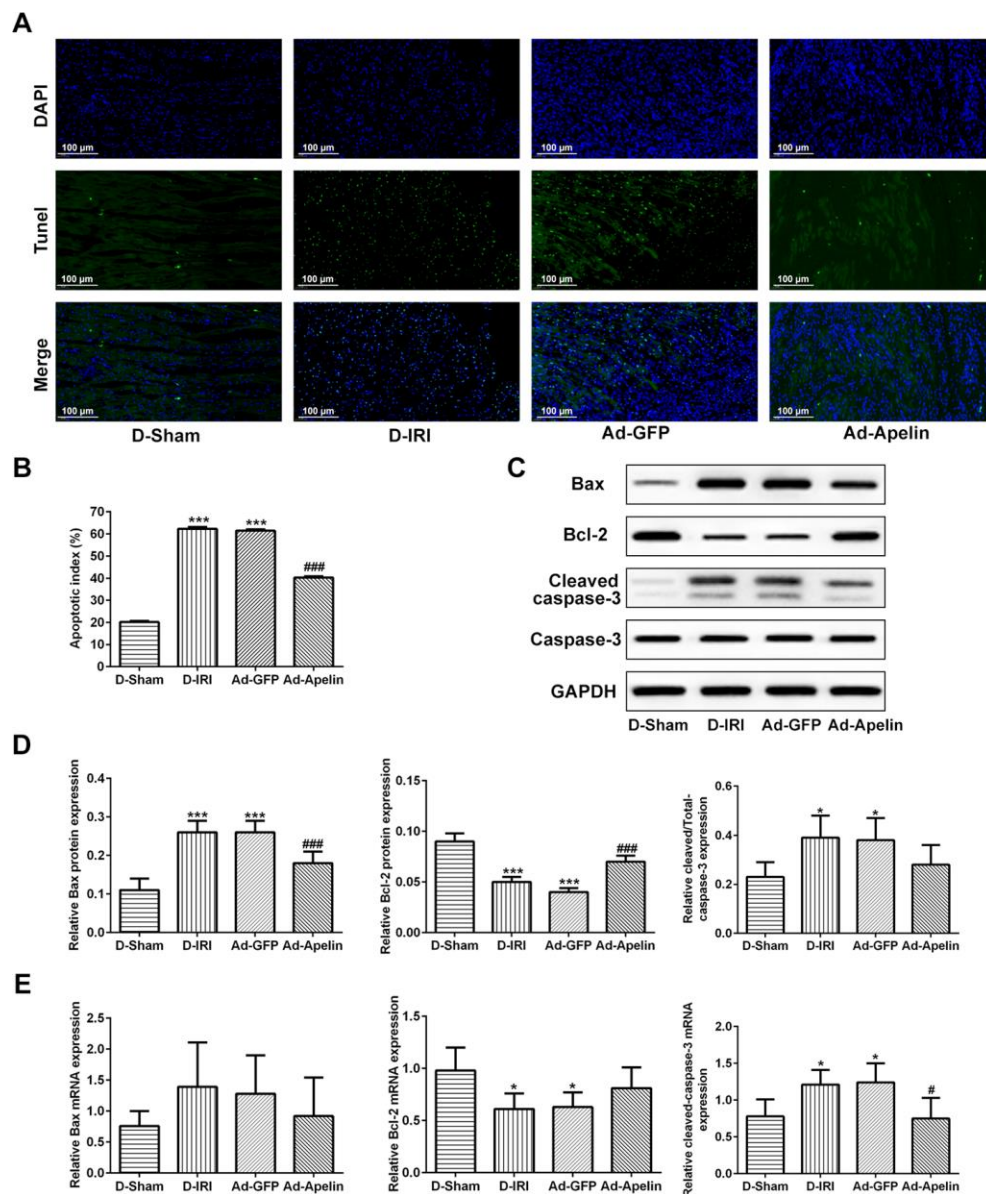According to the observation of echocardiographic measurements and cardiac hemodynamic measurements,

Figure 6. Observation for the apoptosis reduced by the injection of recombined lentiviral vector expressing Apelin. (**A**, **B**) Apoptosis in myocardium was determined by TUNEL analysis. Scale bar=50 μm. (**C**, **D**) Protein levels and analysis of Bcl-2, Bax, and cleaved caspase-3 detecting by western blot assay. (**E**) mRNA levels of Bcl-2, Bax, and cleaved caspase-3 detecting by RT-qPCR. *P<0.05, ***P<0.001 represent the values compared to the D-Sham group. ###P<0.001 represents the values compared to Ad-GFP group. D-Sham: Diabetes sham group; D-IRI: Diabetes ischemia reperfusion injury; Ad-GFP: D-IRI rats injected with Ad-recombined lentiviral vector expressing GFP. Ad-Apelin: D-IRI rats injected with Ad-recombined lentiviral rector expressing Apelin.

we discovered that the exogenously expressed Apelin significantly improved the cardiac functions. Meanwhile, the ischemia reperfusion injury size and heart weight index were significantly decreased under Apelin treatment. The above results suggested that the enhanced levels of Apelin in cardiac tissues might be a kind of compensatory mechanism for the cardiovascular diseases [37].

Actually, multiple mechanisms of the diabetic myocardial ischemia reperfusion injury have been clarified, and many biomarkers for the prognosis of IRI in diabetes patients have also been discovered [38–40]. The peroxisome-proliferator-activated receptors (PPARs) are gene transcriptional regulators, which could be activated and modulate the transcription of many genes associated with insulin effects. The PPARs mainly regulate the lipid metabolism, anti-oxidant defense, mitochondrial biogenesis, endothelial cell metabolism, and also play protective functions in cardiovascular diseases, atherosclerosis, inflammatory diseases, among others [41, 42]. Chen et al. [43] found that the PPAR functions in many biological processes of the cardiovascular system, and antagonizes the hypertension and heart failure. In this work, the PPARα levels were significantly enhanced under treatment with the Apelin, suggesting that the PPAR plays a critical role in the rescue of the cardiac function in D-IRI rats and may be an important mechanism of anti-heart failure in D-IRI rats.

In order to investigate the effects of Apelin on the apoptosis of cardiac tissues, the Bax, Bcl-2 and cleaved caspase-3, were detected in the Apelin overexpression rats and control rats. The results unmasked that Apelin addition significantly enhanced Bcl-2 levels and decreased Bax and cleaved caspase-3 levels, hinting that the Apelin could inactivate apoptosis. However, the apoptotic pathways always involve some of the biomarkers and molecules. The previous studies [44, 45] also elucidated that the oxidative stress together with some of its producers, such as reactive oxygen species (ROS), reactive nitrogen species (RNS), oxidases (NOXs), endothelial nitric oxide synthase [46], is associated with the major pathological progressions of the heart failure, ischemia-reperfusion injury and the cardiac hypertrophy. Except for the above biomarkers, several signaling transduction pathways, such as PI3K/Akt pathway [47], p38MAPK [48] and PI3K pathway [49], also participate in the cardiovascular diseases. In the present study, the overexpression of Apelin in D-IRI rats significantly enhanced the levels of PI3K and eNOS levels, and the production of the NO was also observed in D-IRI rats compared to the rats without Apelin treatment. We speculated that the Apelin enhanced the expression of PI3K and eNOS protein, thus triggering the production of NO. The increased NO levels could lead to the blood vessel diastolic and decrease the blood pressure. Moreover, the overexpression of Apelin also hindered the p38MAPK expression and decreased the apoptotic index in D-IRI rats.

Taken together, these data demonstrated that the Apelin overexpression protects against the diabetic myocardial ischemia reperfusion injury by inhibiting apoptosis and oxidative stress via PI3K and p38MAPK pathway in diabetic IRI rats. These findings provide critical new insight into the knowledge of Apelin's cardio-protective effects, and may develop a novel therapeutic strategy for the diabetic myocardial ischemia reperfusion injury
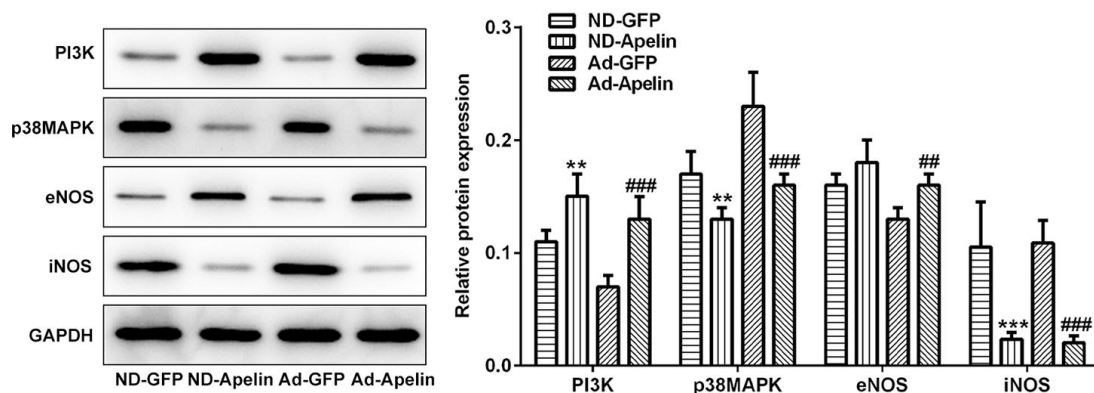

Figure 7. Examination for expression of PI3K, eNOS, iNOS and p38MAPK. (**A**) The blotting bands and statistical analysis for PI3K, p38MAPK, eNOS and iNOS expression examined by western blot assay. $^{**}P<0.01$, $^{***}P<0.001$ represent the values compared to the ND-GFP group. $^{##}P<0.01$, $^{###}P<0.001$ represent the values compared to the Ad-GFP group. ND-GFP: Non-diabetes ischemia reperfusion injury rats injected with recombind lentiviral vector expressing GFP; ND-Apelin: Non-diabetes ischemia reperfusion injury rats injected with Ad-recombined lentiviral rector expressing Apelin; Ad-GFP: Diabetes ischemia reperfusion injury rats injected with Ad-recombind lentiviral vector expressing GFP. Ad-Apelin: Diabetes ischemia reperfusion injury rats injected with Ad-recombind lentiviral rector expressing Apelin.

patients. However, the mechanistic study, such as the PI3K inhibitor or P38 activator delivered in Apelin-treated D-IRI group, needs to be further strengthened in the following investigation, which is a limitation of the present study.

MATERIALS AND METHODS

Reagents and materials

Adult male Sprague-Dawley (SD) rats (body weight 200~270g) were purchased from Experimental Animal Center of Zhengzhou University, Zhengzhou, China. All rats were kept in individual cages under the controlled ambient temperature of 25 ± 2° C and humidity of 50 ± 5%. All rats were housed in a controlled pathogen free environment in a 12-h light-dark cycle. The rats were used to establish the animal models of DM, myocardial IRI and DM complicated with IRI, which would be applied in the following experiments. Male SD rats were randomly divided in two groups, the DM group and non-DM group. All experiments were performed according to the Guidelines of the Institutional Animal Care and approved by the Ethics committee of the Zhengzhou University, Zhengzhou, China.

Type 2 diabetic mellitus (T2DM) rat model

The T2DM model was constructed by high-fat diet (HFD) and streptozotocin (STZ) injection, according to the previously published article [50], with a few modifications. Male SD rats were fed with HFD containing 62% basic fed, 15% cooked lard, 2% sugar, 8% whole milk powder, 8% hen yolk powder, 4% casein and 1% saline for 6 weeks. 30 mg/kg (Sigma-Aldrich, St. Louis, MO, USA) STZ (dissolved in the 0.1 mol/L citric acid, and adjusted to pH 4.2) was injected into the rats (fasting for 12 h) via intraperitoneal injection for one-time after 6 weeks of HFD feeding. The rats were given HFD continuously till the eighth week. Rats with fasting plasma glucose (FPG) levels after STZ injection more than 7.0 mmol/L and /or at 2 h time-point of PG more than 11.1 mmol/L were considered as T2DM model rats. There were 45 rats as the T2DM model rats in this study.

Myocardial ischemia/reperfusion (IR) injury model

The normal rats and the T2DM rats were randomly and respectively divided into two groups, one is for IR injury model (D-IRI, n=14; ND-IRI, n=13) and another for Sham group (D-Sham, n=7; ND-Sham, n=8). The Apelin administration for IR model was divided into two groups, one is Ad-GFP control (n=6) and the other is Ad-Apelin (n=6). The IRI rats were anesthetized by using the ketamine hydrochloride (70 mg/kg) via intraperitoneal injection (i.p), and then the rats were fastened in a supine position. The rats were mechanically ventilated with air through a rodent ventilator followed by oral endotracheal intubation. The body temperature of the rats kept at 37 ± 0.5° C. The thoracic cavity was opened between the fourth and the fifth intercostal of the left edge of the thoracotomy, and the heart of the rat was exposed after pericardial incision. A 7-0 silk thread was sutured around the left anterior descending coronary artery of the rat, 2 mm from the tip of the left auricle. Ten minutes later, when the thread was clamped and tightened, a snare blocking the artery was formed. After ligation, regional epicardial cyanosis in the heart symbolized the successful ischemia. Sixty minutes after the ischemia, the coronary artery reperfusion was performed by releasing the clamp for 1 h. Meanwhile, the Sham-operated animals were performed with the same surgical procedures, although the suture was not fastened. The rat chests were closed post the reperfusion step by step [51]. When the spontaneous breathing of rats was recovered, the breathing machine was removed. These rats were fed at the temperature of 25 ± 2° C and humidity of 50 ± 5%.

Ultrasound measurements

After intervention, echocardiographic analysis was performed to detect the hypertrophic degree of heart with rats in a supine position. Rats were anesthetized by injecting 10% chloral hydrate. Then, the rats were placed on the isothermal pad at the temperature of 40° C. The liner array ultrasound transducer probe (9.0 Hz) was employed to examine the echocardiographic recordings. The long axis views from the left ventricle (LV) were obtained to measure the left ventricular internal diastolic diameter (LVIDd), left ventricular internal dimension systole (LVIDs); the short axis views were used to examine left ventricular posterior wall depth at end-diastole (LVPWd) and left ventricular posterior wall depth at end-systole (LVPWs); left ventricular septal depth at end-diastolic (LVSd), left ventricular septal depth at end-systole (LVSs); ejection fraction (EF, %) and fractional shortening (FS, %) were calculated according to CUBED formula, as previously described [52]. All measurements were repeated three times from at least 10 consecutive cardiac cycles, as the recommendations of American Society of Echocardiography described [53].

Cardiac hemodynamic evaluations

During surgery, the LabScribe software was applied to record and analyze hemodynamic parameters including LV peak systolic pressure (LVSP), the largest upstroke

or descendent velocity of the LV pressure (±dp/dt max) and LV end-diastolic pressure (LVEDP). The LV hemodynamics data was obtained by using the pressure volume catheter following the previously published study [54]. In brief, the right-side carotid artery was cannulated by using the pressure volume catheter after anesthesia (i.p. with the ethyl carbamate, 0.75 g/kg, and α2 chloralose, 70 mg/kg). Then, the tip of the pressure volume catheter was inserted into the left side ventricle via the aorta.

Infarct size measurement

The heart was rapidly excised and frozen at -20° C after the cardiac hemodynamic measurements. Then the frozen heart was cut into 2 mm thick sections. Slices were incubated in the 0.1% triphenyltetrazoliu chloride (TTC) for 10 min at 37° C in phosphate buffer (pH 7.4). The stained slices were subsequently fixed by using the 10% formaldehyde for one night and scanned according to the previous paper [55]. TTC-unstained pale area (infarct area, IA) and TTC-stained red area (ischemic but viable myocardium, IV) were evaluated through planimetry with the image analysis software. Myocardial infarct size was detected as the percent of infarct area over total myocardium area (IV% = IV/(IA+IV) ×100%).

NT-proBNP examination

The blood samples for examination of the NT-proBNP were collected by venipuncture. The blood samples were centrifugated at the speed of 3000 r/min for 10 min at 4° C to obtain the serum, which was shock-frozen and stored at the temperature of -80° C. Then NT-proBNP levels were measured utilizing the electrochemiluminescence immunoassay (ECLIA) and NT-proBNP detection kit (Roche, USA), and detected with the Roche Elec sys 2010 (Roche, USA). The lower to upper limit of the rats were 5 to 35000 pg/ml.

Terminal deoxynucleotidyl transferase-mediated dUTP nick end labeling (TUNEL) staining

The TUNEL staining could examine the 3'-OH terminals of damaged DNA in late apoptosis cells. Therefore, the TUNEL was used to observe apoptosis level in the myocardial infarct size of rats. The TUNEL assay was performed by utilizing the TUNEL-POD kit (Roche, Germany), as previously described [56]. Briefly, the isolated myocardial tissues were embedded with paraffin and sectioned into slices soaked and washed by xylene and hydrated in gradient alcohol. Then the paraffin section of myocardial tissues was treated by proteinase K working solution for 30 min, with PBS washing for three times (3 min/wash). The

3% H_2O_2 solution was used to inactivate the endogenous peroxidase in the myocardial tissues for 10 min, with three times (3 min/wash) of PBS rinse. The paraffin section was treated with TUNEL reaction mixture (biotin dUTP and terminal deoxynucleotidyl transferase (TdT)) in a dark box at 37° C for 1 h, washed by PBS three times. An equal volume of solution with biotin dUTP to replace the TUNEL reaction mixture was used as the negative control. Samples were analyzed under fluorescence microscope (Olympus, Japan) using an excitation wavelength in the range of 450 nm and detection in the range of 565 nm.

Recombined lentiviral vector of Apelin and therapeutic trial

The high titer recombined lentiviral vector was purchased from Ben Yuan Zheng Yang Bio. Co. Inc. (Beijing, China). Meanwhile, the recombined lentiviral vector carrying Apelin and control-GFP were established by Ben Yuan Zheng Yang Bio. Co. Inc. (Beijing, China). D-IRI rats, which was divided into three groups, including D-IRI control group (normal saline (500 µl) via tail vein injection), Ad-GFP group (Ad-GFP vector (500 µl) via tail vein injection) and Ad-Apelin group (Ad-Apelin vector (500 µl) via tail vein injection). The tail vein injection of lentiviral vector carrying Apelin and control-GFP were given 24 h and 14 days after the IR surgery.

Reverse transcription-quantitative polymerase chain reaction (RT-qPCR) analysis

The total RNA was extracted from the myocardium by utilizing TRIzol reagent (Invitrogen, CA, USA). In brief, the myocardium was lysed with TRIzol reagent (1 ml). Then, the isolated RNA was extracted with 200 µl chloroform (Invitrogen, CA, USA), and supernatants were stored for following experiments. The isopropanol (1 ml) was used to precipitate the RNA, following with washing in 70% ethanol for two times. Then, the RNA precipitations were dissolved in diethy pyrocarbonate (DEPC) pre-treated water. Consequently, the promising cDNAs were synthesized by utilizing the Reverse Transcription System (Promega, USA) and AMV reverse transcription enzyme (Promega, USA), RNase inhibitor and ddH$_2$O, 1 µg of total tissue RNA. The reverse transcription condition was listed as below: 85° C for 35 min, 4° C for 10 min.

The RT-qPCR and analysis for the Bax, Bcl-2, cleaved caspase-3 and GAPDH amplification were performed according to previous researches [57, 58]. The primers for Bax, Bcl-2, cleaved caspase-3 and GAPDH were listed in Table 5 and cDNA was used as the template. The forward and reverse primers, 2×SYBR Green

Table 5. The gene sequences for the RT-qPCR amplification.

Genes		Sequences
Bax	Forwards	5'-TTTGTTACAGGGTTTCATCCAGG-3'
	Reverse	5'-GCTAGTGTCTGCCATGTA TT-3'
Bcl-2	Forwards	5'-GGGATACTGGAGATGAAGACT-3'
	Reverse	5'-CCCACCGAAC TCAAAGAAGG-3'
cleaved caspase-3	Forwards	5'-GCTGAACTGEGGTATTGAG-3'
	Reverse	5'-CCTGGAACATCGGATTTGATT-3'
GAPDH	Forwards	5'-CCATCACCATCTTC C AGGAG-3'
	Reverse	5'- CCTGCTTCACCTTCTTG-3'

Mixture (Invitrogen, USA), cDNA and ddH2O were used for the RT-qPCR amplification. The conditions of PCR reaction included pre-denaturation at 94° C for 2 min, denaturation at 94° C for 20 s, annealing at 55-58° C for 40 s, extension at 72° C for 40 s for 32 cycles and extension at 72° C for 2 min. The RT-qPCR assay was conducted on the PCT-100 PCR cycler (MJ Co. Ltd., USA). Each sample was run in triplicate.

Western blot analysis

The expression of Bax, Bcl-2, cleaved caspase-3, PI3K, p38MAPK, eNOS and iNOS was analyzed by western blot analysis, and samples was normalized to GAPDH, as previously described [59–61]. The myocardium were lysed utilizing the RIPA buffer (1 ml/100 mg) at 0° C, and centrifugated at the speed of 12000 r/min for 10 min. The supernatant (40 μg) was loaded to western blot assay by using 15% SDS-PAGE, and was electronic-transferred onto the polyvinylidene fluoride (PVDF) membrane (Dupont, USA). Then, the membranes were blocked utilizing 5% non-fat milk for 2 h at room temperature, followed by wash with PBST buffer for 3 times (5 min/wash). The membranes were incubated with primary antibodies at 4° C for whole night. The membranes were washed with PBST buffer for three times (5 min /time). Then, the membranes were cultivated with AP-labelled goat anti-rabbit IgG and AP-labeled goat anti-mouse IgG (1:10000, Santa Cruz, Co. Ltd. CA, USA) at 37° C for 60 min, and rinsed with PBST buffer for three times (5 min /time). Finally, the membranes were incubated with ECL reagent (Pierce, USA) in the dark for 3 min. The density of bands was evaluated by Image Analysis Software (Bio-Rad Co. Ltd., USA).

ELISA assay for Apelin analysis

The blood samples were collected from the aorta abdominalis, and then formed the mixture with the Trasylol (0.6 TIU/ml). Then the blood samples were centrifugated at 1600 r/min for 15 min at 4° C, and the supernatant was prepared for the ELISA analysis. The serum levels of Apelin was examined by using the commercial Apelin-12 ELISA assay kit (Phoenix pharmaceutical Inc. USA) according to the instruments of the manufacturer.

Immunohistochemistry assay

The immunohistochemistry was employed to assess PPAR-alpha and Apelin expression in the myocardium. The myocardial tissues were fixed utilizing 4% paraformaldehyde continuously for 24 h. Then, the tissues were embedded in paraffin, and sectioned into slices at 4 μm thick by using a rotary microtome. For the immunohistochemistry assay, the endogenous peroxidase was inactivated by incubation with 3% hydrogen peroxide, and slices were blocked by using the 5% BSA for 20 min. Then, the slices were incubated with the rabbit anti-rat PPAR-alpha polyclonal antibody (1:2000 in PBS) (Abcam, UK) at 4° C overnight. Subsequently, the slices were grown with goat anti-rabbit peroxidase-conjugated IgG (1:500 in PBS) (Abcam, UK) at 25° C for 1 h. Briefly, the immunohistochemistry was conducted with the commercial SP immunohistochemistry kit (Zymed, USA). Finally, the slices were immersed in alkaline phosphatase labeled diaminobenzidine (DAB, ZSGB Bio. Inc. Co., Beijing, China), and the images were captured by the inverted fluorescence microscope (Olympus, Japan). Finally, the images were analyzed by utilizing Medical Image Analysis System (HMIAS22000).

Evaluation of collagen volume fraction

The isolation, fixation and the staining for the myocardial biopsy tissues were performed according to the previous study [62]. Among the second half of collected tissue samples, half of them were processed for Masson dye staining. Tissue sections were viewed and photographed using a light microscope (Olympus, Japan). The collagen volume fraction (CVF), an index for the myocardial interstitial fibrosis, was averaged and calculated in the representative areas without the blood

vessel and the endocardium in accordance with the previous report [36]. Percentage of CVF was calculated as the sum of all connective tissue areas divided by the sum of all connective tissues and muscle areas.

Hematoxylin-eosin (HE) staining assessment

After IRI model and Apelin treatment, the hearts were rinsed off the blood, and subsequently immobilized for 48 h. The heart samples were dehydrated using different concentrations of ethanol and embedded in paraffin. The paraffin was cut into slices (5 μm) and stained with HE. IncuCyte™ S3 ZOOM cell imaging system (Essen BioScience, USA) was used to image the staining slices.

Statistical analysis

All of the data in this study were analyzed with use of the SPSS software 13.0 (SPSS Inc., Chicago, Ull, USA). The data were described as mean ± standard deviation, which were gained from at least three independent experiments. The Student's t test and one-way ANOVA was used for the statistical analysis. NT-proBNP expression was presented by median (range) and analyzed by using Kruskal-Wallis. The P value less than 0.05 meant that the difference was significant.

AUTHOR CONTRIBUTIONS

Songtao An and Xi Wang searched the literature, collected the data, conceived and designed the experiments of the current study. Songtao An, Huairui, Shi, Xueqiang Zhang and Hua Meng performed the experiments. Wenbo Li and Dongchang Chen analyzed the data and wrote the manuscript. Junbo Ge revised the manuscript. All authors read and approval the final manuscript.

CONFLICTS OF INTEREST

FUNDING

REFERENCES

1. Kupai K, Szabó R, Veszelka M, Awar AA, Török S, Csonka A, Baráth Z, Pósa A, Varga C. Consequences of exercising on ischemia-reperfusion injury in type 2 diabetic Goto-Kakizaki rat hearts: role of the HO/NOS system. Diabetol Metab Syndr. 2015; 7:85. https://doi.org/10.1186/s13098-015-0080-x PMID:26448786

2. Yin X, Zheng Y, Zhai X, Zhao X, Cai L. Diabetic inhibition of preconditioning- and postconditioning-mediated myocardial protection against ischemia/reperfusion injury. Exp Diabetes Res. 2012; 2012:198048. https://doi.org/10.1155/2012/198048 PMID:21822424

3. Braunwald E, Kloner RA. Myocardial reperfusion: a double-edged sword? J Clin Invest. 1985; 76:1713–19. https://doi.org/10.1172/JCI112160 PMID:4056048

4. Hausenloy DJ, Yellon DM. Targeting myocardial reperfusion injury—the search continues. N Engl J Med. 2015; 373:1073–75. https://doi.org/10.1056/NEJMe1509718 PMID:26321104

5. Ibarra-Lara L, Sánchez-Aguilar M, Hong E, del Valle-Mondragón L, Soria-Castro E, Pérez-Severiano F, Torres-Narváez JC, Ramírez-Ortega M, Pastelín-Hernández GS, Cervantes-Pérez LG, Sánchez-Mendoza A. PPARα stimulation modulates myocardial ischemia-induced activation of renin-angiotensin system. J Cardiovasc Pharmacol. 2015; 65:430–37. https://doi.org/10.1097/FJC.0000000000000186 PMID:25658458

6. Yoshida K, Kobayashi N, Ohno T, Fukushima H, Matsuoka H. Cardioprotective effect of angiotensin II type 1 receptor antagonist associated with bradykinin-endothelial nitric oxide synthase and oxidative stress in dahl salt-sensitive hypertensive rats. J Hypertens. 2007; 25:1633–42. https://doi.org/10.1097/HJH.0b013e32814db89f PMID:17620960

7. Oidor-Chan VH, Hong E, Pérez-Severiano F, Montes S, Torres-Narváez JC, Del Valle-Mondragón L, Pastelín-Hernández G, Sánchez-Mendoza A. Fenofibrate plus metformin produces cardioprotection in a type 2 diabetes and acute myocardial infarction model. PPAR Res. 2016; 2016:8237264. https://doi.org/10.1155/2016/8237264 PMID:27069466

8. Sowers JR. Insulin resistance and hypertension. Am J Physiol Heart Circ Physiol. 2004; 286:H1597–602. https://doi.org/10.1152/ajpheart.00026.2004 PMID:15072967

9. Tatemoto K, Hosoya M, Habata Y, Fujii R, Kakegawa T, Zou MX, Kawamata Y, Fukusumi S, Hinuma S, Kitada C, Kurokawa T, Onda H, Fujino M. Isolation and characterization of a novel endogenous peptide ligand for the human APJ receptor. Biochem Biophys Res Commun. 1998; 251:471–76. https://doi.org/10.1006/bbrc.1998.9489 PMID:9792798

10. Sharma AM, Chetty VT. Obesity, hypertension and insulin resistance. Acta Diabetol. 2005 (Suppl 1); 42:S3–8.
https://doi.org/10.1007/s00592-005-0175-1
PMID:15868117

11. Wu H, Cheng XW, Hao C, Zhang Z, Yao H, Murohara T, Dai Q. Regulation of apelin and its receptor expression in adipose tissues of obesity rats with hypertension and cultured 3T3-L1 adipocytes. Exp Anim. 2014; 63:257–67.
https://doi.org/10.1538/expanim.63.257
PMID:24770651

12. Gurzu B, Petrescu BC, Costuleanu M, Petrescu G. Interactions between apelin and angiotensin II on rat portal vein. J Renin Angiotensin Aldosterone Syst. 2006; 7:212–16.
https://doi.org/10.3317/jraas.2006.040
PMID:17318790

13. Boustany CM, Bharadwaj K, Daugherty A, Brown DR, Randall DC, Cassis LA. Activation of the systemic and adipose renin-angiotensin system in rats with diet-induced obesity and hypertension. Am J Physiol Regul Integr Comp Physiol. 2004; 287:R943–49.
https://doi.org/10.1152/ajpregu.00265.2004
PMID:15191907

14. Medhurst AD, Jennings CA, Robbins MJ, Davis RP, Ellis C, Winborn KY, Lawrie KW, Hervieu G, Riley G, Bolaky JE, Herrity NC, Murdock P, Darker JG. Pharmacological and immunohistochemical characterization of the APJ receptor and its endogenous ligand apelin. J Neurochem. 2003; 84:1162–72.
https://doi.org/10.1046/j.1471-4159.2003.01587.x
PMID:12603839

15. Boucher J, Masri B, Daviaud D, Gesta S, Guigné C, Mazzucotelli A, Castan-Laurell I, Tack I, Knibiehler B, Carpéné C, Audigier Y, Saulnier-Blache JS, Valet P. Apelin, a newly identified adipokine up-regulated by insulin and obesity. Endocrinology. 2005; 146:1764–71.
https://doi.org/10.1210/en.2004-1427
PMID:15677759

16. Sörhede Winzell M, Magnusson C, Ahrén B. The apj receptor is expressed in pancreatic islets and its ligand, apelin, inhibits insulin secretion in mice. Regul Pept. 2005; 131:12–17.
https://doi.org/10.1016/j.regpep.2005.05.004
PMID:15970338

17. Ishida J, Hashimoto T, Hashimoto Y, Nishiwaki S, Iguchi T, Harada S, Sugaya T, Matsuzaki H, Yamamoto R, Shiota N, Okunishi H, Kihara M, Umemura S, et al. Regulatory roles for APJ, a seven-transmembrane receptor related to angiotensin-type 1 receptor in blood pressure in vivo. J Biol Chem. 2004; 279:26274–79.
https://doi.org/10.1074/jbc.M404149200
PMID:15087458

18. Sato T, Suzuki T, Watanabe H, Kadowaki A, Fukamizu A, Liu PP, Kimura A, Ito H, Penninger JM, Imai Y, Kuba K. Apelin is a positive regulator of ACE2 in failing hearts. J Clin Invest. 2013; 123:5203–11.
https://doi.org/10.1172/JCI69608 PMID:24177423

19. Sabry MM, Mahmoud MM, Shoukry HS, Rashed L, Kamar SS, Ahmed MM. Interactive effects of apelin, renin-angiotensin system and nitric oxide in treatment of obesity-induced type 2 diabetes mellitus in male albino rats. Arch Physiol Biochem. 2019; 125:244–54.
https://doi.org/10.1080/13813455.2018.1453521
PMID:29564917

20. Zhou Q, Cao J, Chen L. Apelin/APJ system: a novel therapeutic target for oxidative stress-related inflammatory diseases (review). Int J Mol Med. 2016; 37:1159–69.
https://doi.org/10.3892/ijmm.2016.2544
PMID:27035220

21. Wang W, McKinnie SM, Patel VB, Haddad G, Wang Z, Zhabyeyev P, Das SK, Basu R, McLean B, Kandalam V, Penninger JM, Kassiri Z, Vederas JC, et al. Loss of apelin exacerbates myocardial infarction adverse remodeling and ischemia-reperfusion injury: therapeutic potential of synthetic apelin analogues. J Am Heart Assoc. 2013; 2:e000249.
https://doi.org/10.1161/JAHA.113.000249
PMID:23817469

22. Kumagai S, Nakayama H, Fujimoto M, Honda H, Serada S, Ishibashi-Ueda H, Kasai A, Obana M, Sakata Y, Sawa Y, Fujio Y, Naka T. Myeloid cell-derived LRG attenuates adverse cardiac remodelling after myocardial infarction. Cardiovasc Res. 2016; 109:272–82.
https://doi.org/10.1093/cvr/cvv273 PMID:26678356

23. Azizi Y, Faghihi M, Imani A, Roghani M, Zekri A, Mobasheri MB, Rastgar T, Moghimian M. Post-infarct treatment with [Pyr(1)]apelin-13 improves myocardial function by increasing neovascularization and overexpression of angiogenic growth factors in rats. Eur J Pharmacol. 2015; 761:101–08.
https://doi.org/10.1016/j.ejphar.2015.04.034
PMID:25936512

24. Joseph JJ, Donner TW. Long-term insulin glargine therapy in type 2 diabetes mellitus: a focus on cardiovascular outcomes. Vasc Health Risk Manag. 2015; 11:107–16.
https://doi.org/10.2147/VHRM.S50286
PMID:25657589

25. Shi Z, Fu F, Yu L, Xing W, Su F, Liang X, Tie R, Ji L, Zhu M, Yu J, Zhang H. Vasonatrin peptide attenuates myocardial ischemia-reperfusion injury in diabetic rats

and underlying mechanisms. Am J Physiol Heart Circ Physiol. 2015; 308:H281–90.
https://doi.org/10.1152/ajpheart.00666.2014
PMID:25485902

26. Baumgardt SL, Paterson M, Leucker TM, Fang J, Zhang DX, Bosnjak ZJ, Warltier DC, Kersten JR, Ge ZD. Chronic co-administration of sepiapterin and l-citrulline ameliorates diabetic cardiomyopathy and myocardial ischemia/reperfusion injury in obese type 2 diabetic mice. Circ Heart Fail. 2016; 9:e002424.
https://doi.org/10.1161/CIRCHEARTFAILURE.115.002424 PMID:26763290

27. Kraegen EW, James DE, Bennett SP, Chisholm DJ. In vivo insulin sensitivity in the rat determined by euglycemic clamp. Am J Physiol. 1983; 245:E1–7.
https://doi.org/10.1152/ajpendo.1983.245.1.E1
PMID:6346896

28. Schannwell CM, Schneppenheim M, Perings S, Plehn G, Strauer BE. Left ventricular diastolic dysfunction as an early manifestation of diabetic cardiomyopathy. Cardiology. 2002; 98:33–39.
https://doi.org/10.1159/000064682 PMID:12373045

29. Yazici D, Yavuz DG, Toprak A, Deyneli O, Akalin S. Impaired diastolic function and elevated nt-proBNP levels in type 1 diabetic patients without overt cardiovascular disease. Acta Diabetol. 2013; 50:155–61.
https://doi.org/10.1007/s00592-010-0235-z
PMID:21072546

30. Bjurman C, Petzold M, Venge P, Farbemo J, Fu ML, Hammarsten O. High-sensitive cardiac troponin, NT-proBNP, hFABP and copeptin levels in relation to glomerular filtration rates and a medical record of cardiovascular disease. Clin Biochem. 2015; 48:302–07.
https://doi.org/10.1016/j.clinbiochem.2015.01.008
PMID:25637776

31. Budweiser S, Luchner A, Jörres RA, Heinemann F, Hitzl AP, Schmidbauer K, Riegger G, Pfeifer M. NT-proBNP in chronic hypercapnic respiratory failure: a marker of disease severity, treatment effect and prognosis. Respir Med. 2007; 101:2003–10.
https://doi.org/10.1016/j.rmed.2007.04.001
PMID:17532200

32. Dominic EA, Ramezani A, Anker SD, Verma M, Mehta N, Rao M. Mitochondrial cytopathies and cardiovascular disease. Heart. 2014; 100:611–18.
https://doi.org/10.1136/heartjnl-2013-304657
PMID:24449718

33. França CN, Izar MC, Amaral JB, Tegani DM, Fonseca FA. Microparticles as potential biomarkers of cardiovascular disease. Arq Bras Cardiol. 2015; 104:169–74.
https://doi.org/10.5935/abc.20140210
PMID:25626759

34. Wang HH, Li PC, Huang HJ, Lee TY, Lin CY. Peritoneal dialysate effluent during peritonitis induces human cardiomyocyte apoptosis by regulating the expression of GATA-4 and Bcl-2 families. J Cell Physiol. 2011; 226:94–102.
https://doi.org/10.1002/jcp.22309 PMID:20625998

35. Dai J, Liu H, Zhou J, Huang K. Selenoprotein R protects human lens epithelial cells against d-galactose-induced apoptosis by regulating oxidative stress and endoplasmic reticulum stress. Int J Mol Sci. 2016; 17:231.
https://doi.org/10.3390/ijms17020231
PMID:26875981

36. Koguchi W, Kobayashi N, Takeshima H, Ishikawa M, Sugiyama F, Ishimitsu T. Cardioprotective effect of apelin-13 on cardiac performance and remodeling in end-stage heart failure. Circ J. 2012; 76:137–44.
https://doi.org/10.1253/circj.cj-11-0689
PMID:22082814

37. Atluri P, Morine KJ, Liao GP, Panlilio CM, Berry MF, Hsu VM, Hiesinger W, Cohen JE, Joseph Woo Y. Ischemic heart failure enhances endogenous myocardial apelin and APJ receptor expression. Cell Mol Biol Lett. 2007; 12:127–38.
https://doi.org/10.2478/s11658-006-0058-7
PMID:17119870

38. Li H, Liu Z, Wang J, Wong GT, Cheung CW, Zhang L, Chen C, Xia Z, Irwin MG. Susceptibility to myocardial ischemia reperfusion injury at early stage of type 1 diabetes in rats. Cardiovasc Diabetol. 2013; 12:133.
https://doi.org/10.1186/1475-2840-12-133
PMID:24041262

39. Lin J, Wang T, Li Y, Wang M, Li H, Irwin MG, Xia Z. N-acetylcysteine restores sevoflurane postconditioning cardioprotection against myocardial ischemia-reperfusion injury in diabetic rats. J Diabetes Res. 2016; 2016:9213034.
https://doi.org/10.1155/2016/9213034
PMID:26783539

40. El-Sahar AE, Safar MM, Zaki HF, Attia AS, Ain-Shoka AA. Neuroprotective effects of pioglitazone against transient cerebral ischemic reperfusion injury in diabetic rats: modulation of antioxidant, anti-inflammatory, and anti-apoptotic biomarkers. Pharmacol Rep. 2015; 67:901–06.
https://doi.org/10.1016/j.pharep.2015.03.018
PMID:26398383

41. Robinson E, Grieve DJ. Significance of peroxisome proliferator-activated receptors in the cardiovascular system in health and disease. Pharmacol Ther. 2009; 122:246–63.
https://doi.org/10.1016/j.pharmthera.2009.03.003
PMID:19318113

42. Kim T, Yang Q. Peroxisome-proliferator-activated receptors regulate redox signaling in the cardiovascular system. World J Cardiol. 2013; 5:164–74. https://doi.org/10.4330/wjc.v5.i6.164 PMID:23802046

43. Chen R, Liang F, Moriya J, Yamakawa J, Takahashi T, Shen L, Kanda T. Peroxisome proliferator-activated receptors (PPARs) and their agonists for hypertension and heart failure: are the reagents beneficial or harmful? Int J Cardiol. 2008; 130:131–39. https://doi.org/10.1016/j.ijcard.2008.03.080 PMID:18582964

44. Sawyer DB, Siwik DA, Xiao L, Pimentel DR, Singh K, Colucci WS. Role of oxidative stress in myocardial hypertrophy and failure. J Mol Cell Cardiol. 2002; 34:379–88. https://doi.org/10.1006/jmcc.2002.1526 PMID:11991728

45. Takimoto E, Kass DA. Role of oxidative stress in cardiac hypertrophy and remodeling. Hypertension. 2007; 49:241–48. https://doi.org/10.1161/01.HYP.0000254415.31362.a7 PMID:17190878

46. Bamichas G, Natse T, Christidou F, Stangou M, Karagianni A, Koukourikos S, Chaidemenos G, Chrysomallis F, Sombolos K. Plasma exchange in patients with toxic epidermal necrolysis. Ther Apher. 2002; 6:225–28. https://doi.org/10.1046/j.1526-0968.2002.00409.x PMID:12109948

47. Deng C, Sun Z, Tong G, Yi W, Ma L, Zhao B, Cheng L, Zhang J, Cao F, Yi D. A-lipoic acid reduces infarct size and preserves cardiac function in rat myocardial ischemia/reperfusion injury through activation of PI3K/Akt/Nrf2 pathway. PLoS One. 2013; 8:e58371. https://doi.org/10.1371/journal.pone.0058371 PMID:23505496

48. Shafi S, Codrington R, Gidden LM, Ferns GA. Increased expression of phosphorylated forms of heat-shock protein-27 and p38MAPK in macrophage-rich regions of fibro-fatty atherosclerotic lesions in the rabbit. Int J Exp Pathol. 2016; 97:56–65. https://doi.org/10.1111/iep.12167 PMID:26853073

49. Strijdom H, Friedrich SO, Hattingh S, Chamane N, Lochner A. Hypoxia-induced regulation of nitric oxide synthase in cardiac endothelial cells and myocytes and the role of the PI3-K/PKB pathway. Mol Cell Biochem. 2009; 321:23–35. https://doi.org/10.1007/s11010-008-9906-2 PMID:18791856

50. Watts LM, Manchem VP, Leedom TA, Rivard AL, McKay RA, Bao D, Neroladakis T, Monia BP, Bodenmiller DM, Cao JX, Zhang HY, Cox AL, Jacobs SJ, et al. Reduction of hepatic and adipose tissue glucocorticoid receptor expression with antisense oligonucleotides improves hyperglycemia and hyperlipidemia in diabetic rodents without causing systemic glucocorticoid antagonism. Diabetes. 2005; 54:1846–53. https://doi.org/10.2337/diabetes.54.6.1846 PMID:15919808

51. Yang J, Yang J, Ding JW, Chen LH, Wang YL, Li S, Wu H. Sequential expression of TLR4 and its effects on the myocardium of rats with myocardial ischemia-reperfusion injury. Inflammation. 2008; 31:304–12. https://doi.org/10.1007/s10753-008-9079-x PMID:18677579

52. Collins KA, Korcarz CE, Lang RM. Use of echocardiography for the phenotypic assessment of genetically altered mice. Physiol Genomics. 2003; 13:227–39. https://doi.org/10.1152/physiolgenomics.00005.2003 PMID:12746467

53. Sahn DJ, DeMaria A, Kisslo J, Weyman A. Recommendations regarding quantitation in M-mode echocardiography: results of a survey of echocardiographic measurements. Circulation. 1978; 58:1072–83. https://doi.org/10.1161/01.cir.58.6.1072 PMID:709763

54. Zhang Y, Dedkov EI, Teplitsky D, Weltman NY, Pol CJ, Rajagopalan V, Lee B, Gerdes AM. Both hypothyroidism and hyperthyroidism increase atrial fibrillation inducibility in rats. Circ Arrhythm Electrophysiol. 2013; 6:952–59. https://doi.org/10.1161/CIRCEP.113.000502 PMID:24036190

55. Donato M, D'Annunzio V, Berg G, Gonzalez G, Schreier L, Morales C, Wikinski RL, Gelpi RJ. Ischemic postconditioning reduces infarct size by activation of A1 receptors and K+(ATP) channels in both normal and hypercholesterolemic rabbits. J Cardiovasc Pharmacol. 2007; 49:287–92. https://doi.org/10.1097/FJC.0b013e31803c55fe PMID:17513947

56. Xia C, Zhu L, Shao W, Mi S, Du S, Ye L, Liu M, Pang Y, Nong L, Jiang C, Zhao H, Qi G. The effect of hippocampal cognitive impairment and XIAP on glucose and lipids metabolism in rats. Cell Physiol Biochem. 2016; 38:609–18. https://doi.org/10.1159/000438654 PMID:26845572

57. Zhou T, Xiang DK, Li SN, Yang LH, Gao LF, Feng C. MicroRNA-495 ameliorates cardiac microvascular endothelial cell injury and inflammatory reaction by suppressing the NLRP3 inflammasome signaling pathway. Cell Physiol Biochem. 2018; 49:798–815.

https://doi.org/10.1159/000493042
PMID:30165354

58. Livak KJ, Schmittgen TD. Analysis of relative gene expression data using real-time quantitative PCR and the 2(-delta delta C(T)) method. Methods. 2001; 25:402–08.
https://doi.org/10.1006/meth.2001.1262
PMID:11846609

59. Bell RM, Yellon DM. Bradykinin limits infarction when administered as an adjunct to reperfusion in mouse heart: the role of PI3K, Akt and eNOS. J Mol Cell Cardiol. 2003; 35:185–93.
https://doi.org/10.1016/s0022-2828(02)00310-3
PMID:12606259

60. Mukherjee S, Lekli I, Goswami S, Das DK. Freshly crushed garlic is a superior cardioprotective agent than processed garlic. J Agric Food Chem. 2009; 57:7137–44.

https://doi.org/10.1021/jf901301w
PMID:19722587

61. Wu WY, Wang WY, Ma YL, Yan H, Wang XB, Qin YL, Su M, Chen T, Wang YP. Sodium tanshinone IIA silate inhibits oxygen-glucose deprivation/recovery-induced cardiomyocyte apoptosis via suppression of the NF-κB/TNF-α pathway. Br J Pharmacol. 2013; 169:1058–71.
https://doi.org/10.1111/bph.12185
PMID:23517194

62. Aoki T, Fukumoto Y, Sugimura K, Oikawa M, Satoh K, Nakano M, Nakayama M, Shimokawa H. Prognostic impact of myocardial interstitial fibrosis in non-ischemic heart failure. -comparison between preserved and reduced ejection fraction heart failure.-. Circ J. 2011; 75:2605–13.
https://doi.org/10.1253/circj.cj-11-0568
PMID:21821961